Journal of Polymer Research (2018) 25: 242
https://doi.org/10.1007/s10965-018-1634-z

ORIGINAL PAPER

# Thermal stability and decomposition behaviors of segmented copolymer poly(urethane-urea-amide)

Yunyun Yang[1] · Xilei Cao[1] · Hang Luo[1] · Xufu Cai[1]

Received: 20 May 2018 / Accepted: 8 October 2018 / Published online: 26 October 2018


## Abstract

Polyurethane (PU) has become one of the most important segmented copolymers, due to it can be tailored to suit a wide range of application requirements by changing their structures and compositions. Amide, urethane and urea, which are capable of forming intermolecular hydrogen bonding to enhance the microphase separated morphology, are now used to consist segmented copolymers (poly(urethane-urea-amide) PUUA). In order to understand the usage temperature of the material and the protective measures which can be used, we wanted study the thermal stability and degradation process of PUUA. For study the stability of molecule structure, the thermal degradation behaviors of PUUA were extensively investigated with the thermogravimetric analysis (TG) under pure nitrogen and air, firstly. And the degradation activation energy of PUUA was further determined by the Flynn-Wall-Ozawa method. To find the order of thermal stability of bonds, thermogravimeter coupled with FTIR spectrophotometer (TG/FTIR) was used to research their gaseous products and their releasing intensity under nitrogen. In addition, the thermal decomposition behaviors of PUUA under air were also simulated by TG/FTIR. All results demonstrated that the bond of polyurethane decomposed firstly, both under air and nitrogen. And the protection of the bond of polyurethane was beneficial to prolong the service life of PUUA materials.

**Keywords** Segmented copolymers · Poly(urethane-urea-amides) PUUA · Thermal analyses · Gaseous analysis

## Introduction

In general, segmented copolymers consist of an amorphous or low melting polyether or polyester (soft) segment that alternates with a crystalline or high glass transition temperature (hard) segment along the polymer backbone [1–6]. Its special morphology imparts segmented polymers with excellent mechanical properties at high and low temperatures [7, 8]. Among them, polyurethane (PU) are high performance segmented polymers consisting of soft polyether segments and hard polyamide segments [9, 10]. The most important feature is the segmented polymers can be tailored to suit a wide range of application requirements by changing their structures and compositions [11].

In particular, PUs have drawn much attention in many different class of polymers, such as electromechanical applications, biomedical applications, and coatings applications [12, 13]. For example, Chen [14] prepared a series of poly (urethane urea) (PUU) networks by reacting castor oil -based polyurethane precursor with different amounts of 4-aminophenyl disulfide with good mechanical properties and reprocessibility. Rodrigo [15] used aqueous dispersions of poly(urethane-urea) (PUU) to form dense membranes for the permeability and separation of pure $CO_2$, $CH_4$, and $N_2$, at room temperature. Due to the similar reaction groups of polyurethane, polyamide and polyurea, we use amide, urethane and urea to consist segmented copolymers (Poly(urethane-urea-amides) PUUA) which are capable of forming intermolecular hydrogen bonding to enhance the microphase separated morphology. The amide functionality possesses strong hydrogen bonding favorable to the formation of physical crosslinks to enhance the mechanical properties, solvent resistance and thermal and dimensional stability of PUUA [16, 17]. On the other hand, the polyether amorphous segments form a continuous phase contributing to low temperature flexibility and long-range elasticity of the copolymer [18]. Muthu

✉ Xufu Cai
caixf2008@scu.edu.cn

[1] College of Polymer Science and Materials, The State Key Laboratory of Polymer Materials Engineering, Sichuan University, Chengdu 610065, China

[19] got excellent solvent resistivity and thermal stability PUUA by the synthesis of 4,4′ -methylenediphenyl diisocyanate (MDI) based polyurethane-ureas-amide using diamine-diamide chain extenders and dihydroxy polystyrene (PSt). Those works focused on the syntheses and performances of their segmented copolymer. But the thermal stability is also an important factor in the application of PUUAs. So we want to study the thermal stability and decomposition process of PUUA.

In our previous paper [20], we have published the reactive processing and properties of PUUA. For farther use and study, we have researched its thermal stability and decomposition. In this paper, the thermal degradation behaviors of PUUA were extensively investigated with the thermogravimetric analysis (TG) under pure nitrogen and air, firstly. And the degradation activation energy of PUUA was further determined by the Flynn-Wall-Ozawa [21–25] method, according to the results of TG. To find the order of thermal stability of bonds, thermogravimetric analysis coupled with Fourier Transform infrared spectroscopy (TG/FTIR) was used to research their gaseous products and their releasing intensity under nitrogen. In addition, the thermal decomposition behaviors of PUUA under air were also simulated by TG/FTIR.

## Experimental

### Materials

4,4-diphenylmethane diisocyanate (MDI, AR) was supplied by Yantai Wanhua Polyurethane Co. Ltd. (Shandong, China). Polytetramethyleneglycol (PTMG, industrial grade, Mw =1000 g $mol^{-1}$,) was purchased from Hyosung Chemicals Co. Ltd.(Jiaxing, China). $\alpha,\omega$-amino nylon-6 with Mw =1000 g $mol^{-1}$ and deionized water were made in the laboratory. Multiblock copolymer PUUA(Scheme 1) was polymerized in laboratory according to Kong, et al. [20].

### Instrumentation

The measurement of TG was carried out using a Netzsch TG209 F1 thermogravimeter at a linear heating rate of 10 K/min, 20 K/min, 30 K/min and 50 K/min, respectively. About 7–8 mg of each sample was heated in the temperature range from 300 to 1073 K, with a controlled dry nitrogen or air flow of 60 ml/min. The sample was loaded with ceramic crucibles which were treated by high temperature. TG/FTIR measurements were carried out on a Mettler Toledo TG/DSC 1 STAR$^e$ System thermogravimeter coupled with a Nicolet iS10 FTIR spectrophotometer. About 8 mg of each sample was heated from 300 to 1073 K with a heating rate of 10 K/min under pure nitrogen or air condition. The flow of dry nitrogen and air was 60 ml/min. The sample was loaded with ceramic crucibles which were treated by high temperature.

## Results and discussion

### The thermal decomposition behaviors under nitrogen

The mass loss and mass loss rate curves under pure nitrogen were respectively presented in Fig. 1a, b. The temperature of $T_P$ and $R_P$ of PU-PA increased increasingly with the heating rate increasing.

The fundamental rate equation used in all kinetic studies is generally described as

$$d\alpha/dt = k\ f\ (\alpha) \tag{1}$$

where $k$ is the rate constant and f ($\alpha$) is the reaction model, a function depending on the actual reaction mechanism. Equation (1) expresses the rate of conversion, d$\alpha$/dt, at a constant temperature as a function of the reactant concentration loss and rate constant. In this study, the conversion rate a is defined as:

$$\alpha = (W_0 - W_t)/(W_0 - W_f) \tag{2}$$

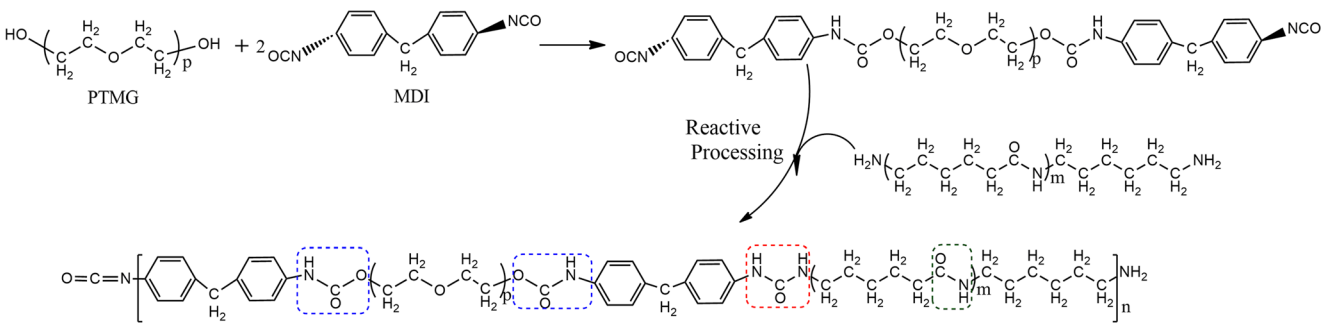


**Scheme 1** The structure of PUUA(in the blue block was bond of polyurethane; in the red block was bond of polyurea; in the green block was bond of polyamide)

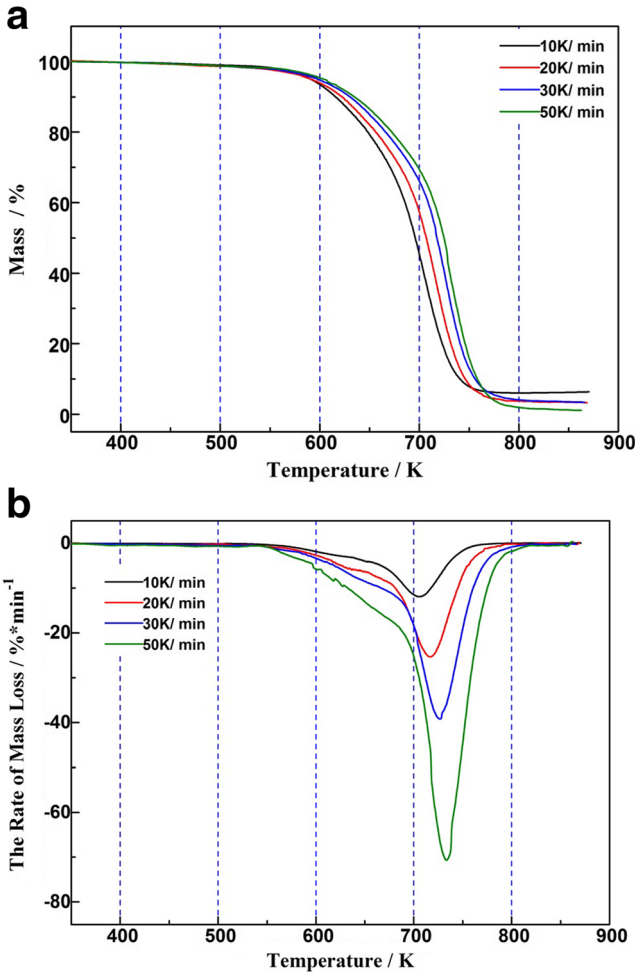


**Fig. 1** The TG curves (**a**) and DTG curves (**b**) of HCTP and N-HCTP under nitrogen

where $W_t$, $W_0$, and $W_f$ are time $t$, initial and final weights of the sample, respectively. The rate constant $k$ is generally given by the Arrhenius equation:

$$k = A\exp(-E/RT) \tag{3}$$

where E is the apparent activation energy (kJ/mol), R is the gas constant (8.314 J/K mol), A is the pre-exponential factor ($min^{-1}$), T is the absolute temperature (K). The combination of Eqs. (1) and (3) gives the following relationship:

$$d\alpha/dt = A\exp(-E/RT)\ f(\alpha) \tag{4}$$

For a dynamic TGA process, introducing the heating rate, $\beta = Dt/dt$, into Eq. (4), Eq. (5) is obtained as:

$$d\alpha/dt = (A/\beta)\exp(-E/RT)\ f(\alpha) \tag{5}$$

Equations (4) and (5) are the fundamental expressions of analytical methods to calculate kinetic parameters on the basis of TGA data.

Flynn-Wall-Ozawa [21–25] method was chosen to study the stability of samples in the entire area of decomposition because it did not require the knowledge of reaction mechanism. To show the activation energy change of decomposition during mass loss, Flynn-Wall-Ozawa method represented a simple method of determining activation energy directly from weight loss versus temperature obtained at several heating rates, using the equation:

$$\frac{d(\log\beta)}{d\left(\frac{1}{T}\right)} = -0.4567\frac{E}{R} \tag{6}$$

$T$ was the temperature of the same mass loss decomposition at the different heating rates and β was the heating rate. Figure 2 showed the trend of PU-PA under nitrogen. The activation energy $E_x$ for different mass loss decomposition values can be calculated from a logβ versus $1/T$ plot.

$$Ex = -2.1896R*(\text{slope of fitting line})$$

As shown in the Fig. 3, the activation energy of PUUA decomposition decreased with the mass loss increasing before 40% mass loss. The activation decomposition energy of PUUA at initial mass loss was 268.9KJ*$mol^{-1}$. The activation decomposition energy of PUUA at 40% mass loss was 212.0KJ*$mol^{-1}$. Then the activation energy of PUUA increased rapidly. The activation decomposition energy of PUUA at 90% mass loss was 382.9KJ*$mol^{-1}$. It indicated that the decomposition activation energy of PUUA decreased because of the change of stability after the initial degradation. After 40% mass loss, the stability of residues increased with the mass loss.

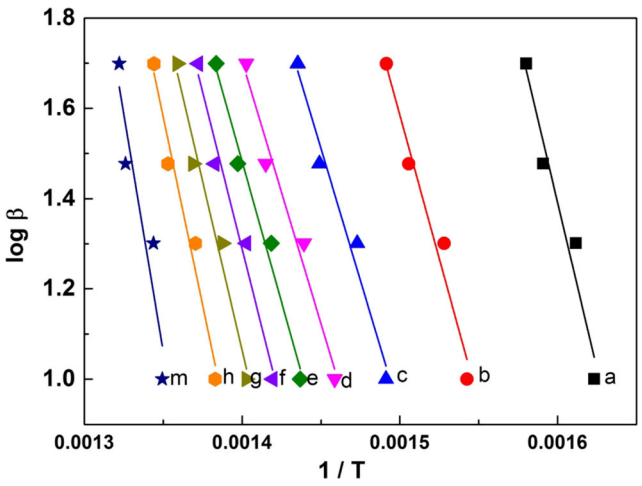


**Fig. 2** The Flynn-Wall-Ozawa values of PU-PA at different heating rates under nitrogen (a:mass loss 10%; b:mass loss 20%; c:mass loss 30%; d:mass loss 40%; e:mass loss 50%; f:mass loss 60%; g:mass loss 70%; h:mass loss 80%; m:mass loss 90%)

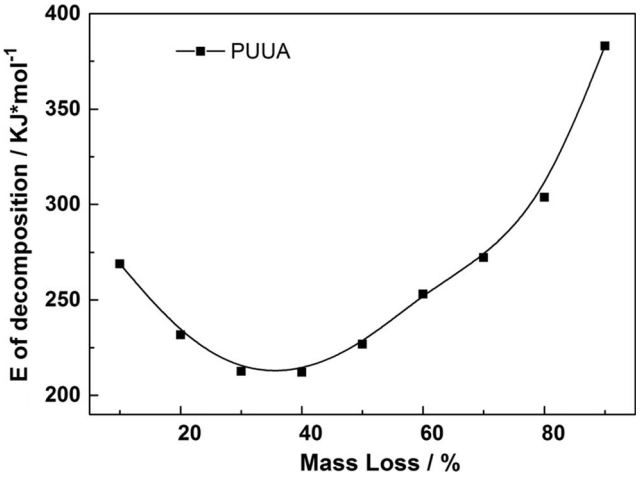


Fig. 3 The activation energy trend curve of PUUA under nitrogen

## The thermal decomposition behaviors under air

At the same time, the thermal stability and decomposition behaviors of PUUA under air was also contrasted by TG analysis. The different heating rate TG and DTG curves of PUUA under air were respectively presented in Fig. 4a, b. The participation of air shifted the onset decomposition temperature of PUUA to low temperature. But the char residues yield of PUUA under air was higher than the char residues yield of PUUA under nitrogen. There were two decomposition peaks of PUUA under air, while there was one decomposition peaks under nitrogen.

Flynn-Wall-Ozawa method was also chosen to study the stability of samples in the entire area of decomposition under air. Figure 5 showed the fitting lines of Flynn-Wall-Ozawa method of PUUA. In Fig. 6, the trend of activation energy was similar with that of PUUA under nitrogen. The activation energy of PUUA decomposition decreased with the mass loss increasing before 20% mass loss. Then the activation energy of PUUA increased rapidly. But the activation energy of PUUA under air varied more than that of PUUA under nitrogen. The difference between the minimum and maximum decomposition energy under air was 366KJ/mol, which was 2.14 times of that under nitrogen. All the difference behaviors under air indicated that the introduction of oxygen accelerated the initial decomposition and catalyzed the production of stable materials.

## The decomposition analysis by TG/FTIR

In this part, the gaseous products generated in the decomposition processing were detected by TG/FTIR. Figure 7 showed the intensity of pyrolysis gaseous of PUUA under nitrogen and air. There was one peak of pyrolysis gaseous of PUUA

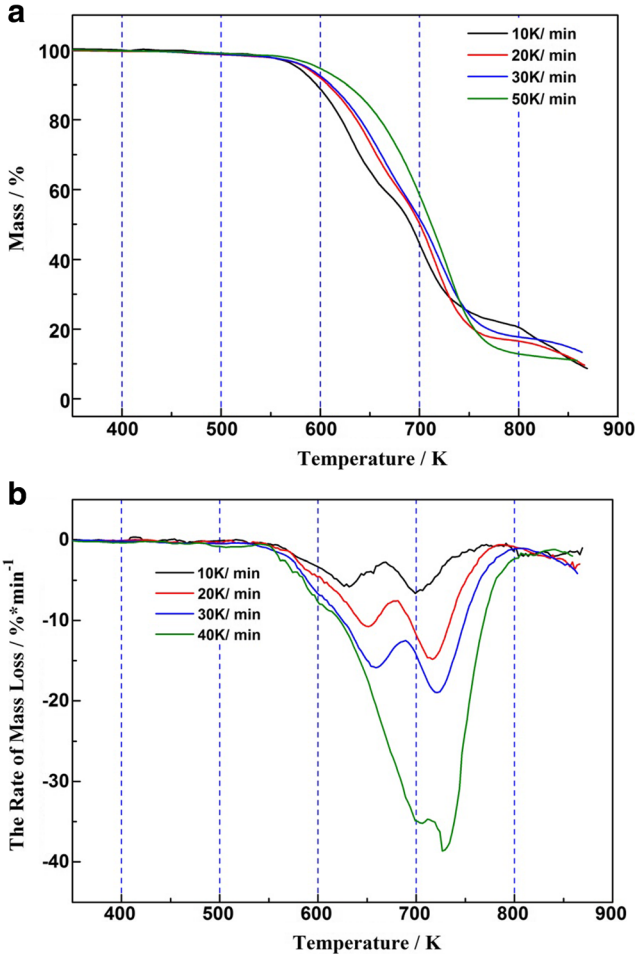


Fig. 4 The TG curves (**a**) and DTG curves (**b**) of PUUA under air

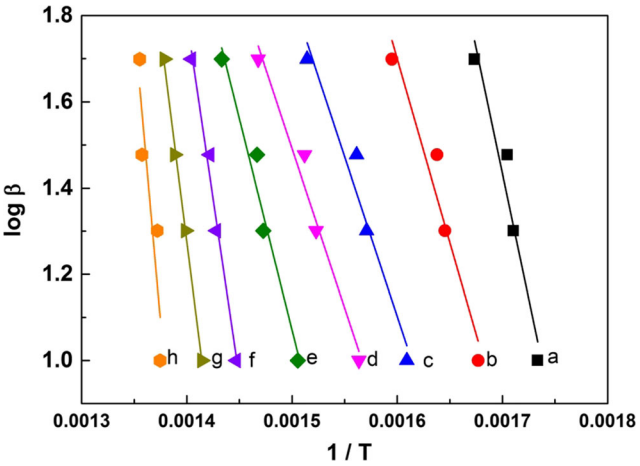


Fig. 5 The Flynn-Wall-Ozawa values of PUUA at different heating rates under air (a:mass loss 10%; b:mass loss 20%; c:mass loss 30%; d:mass loss 40%; e:mass loss 50%; f:mass loss 60%; g:mass loss 70%; h:mass loss 80%)

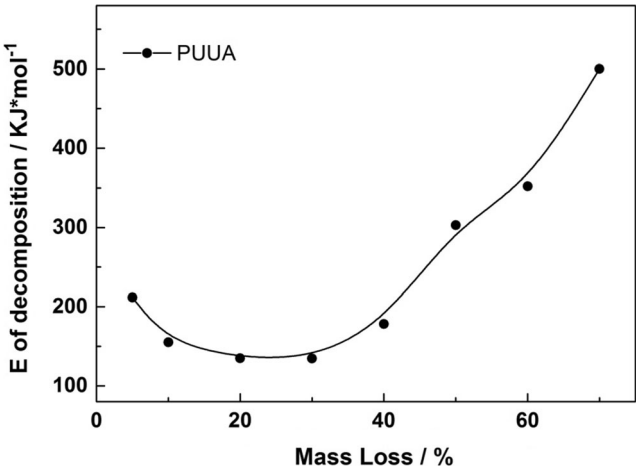


**Fig. 6** The activation energy trend curve of PUUA under air

under nitrogen, while two peaks of PUUA under air. Also the temperature of peaks was consistent with those of DTG curves.

Figure 8 showed the 3-Dimensional FTIR spectra of gaseous products of PUUA under nitrogen and air. As shown in Fig. 8a, c, the FTIR spectra of gaseous products under nitrogen, there were strong intensity peaks at the range of 3600–3400 $cm^{-1}$, 3000-2900 $cm^{-1}$, 2400–2300 $cm^{-1}$ and 1800-1000 $cm^{-1}$. In order to make the FTIR peaks more clearly, we chose some FTIR spectra at different temperature. And the FTIR spectra of gaseous products of PUUA were listed in Fig. 9.

As shown in Figs. 8a, c and 9a, the first peaks of gaseous products were the characteristic peaks of $CO_2$ under nitrogen. The next were the peaks of ether and -$CH_2$-. It suggested that the bond of polyurethane was ruptured firstly. At the same time, there were small peaks of -N-H, which indicated the

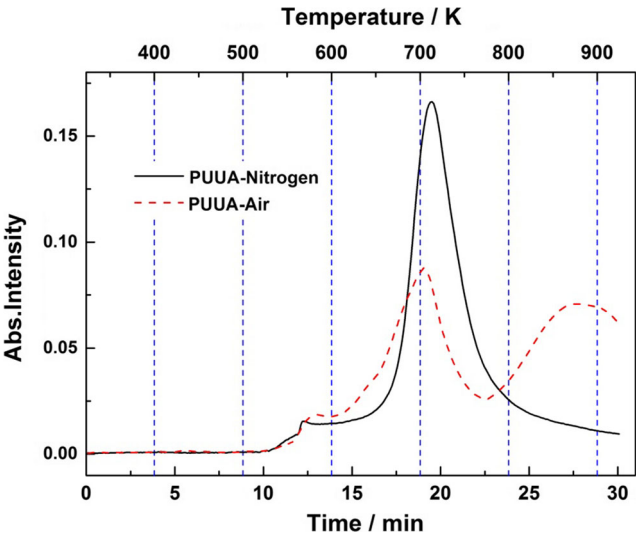


**Fig. 7** The intensity of pyrolysis gaseous of PUUA under nitrogen and air

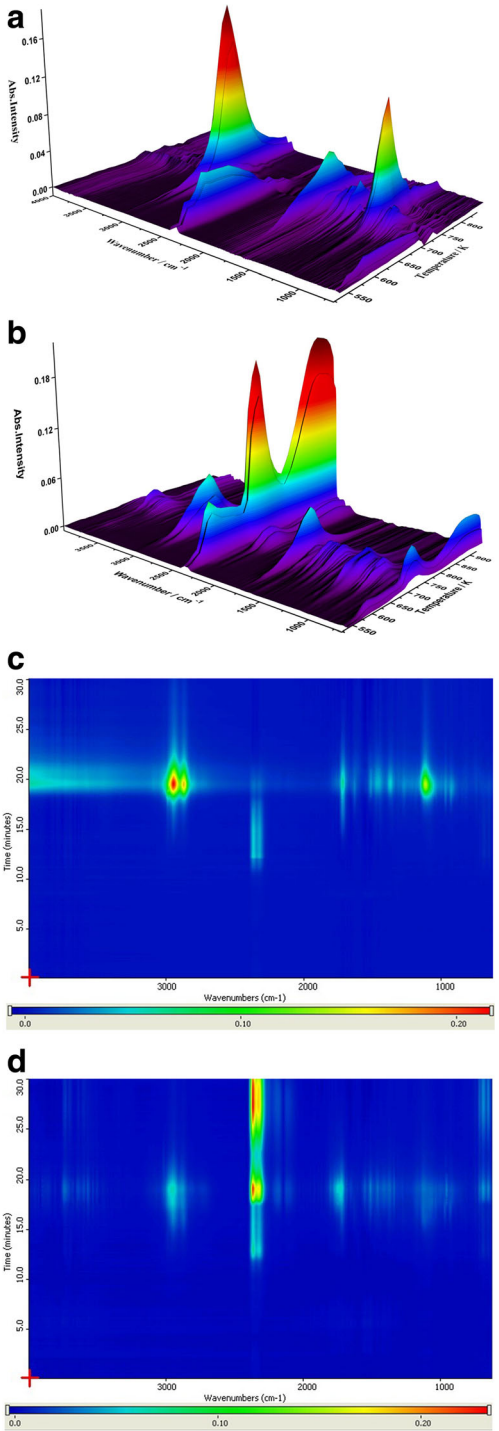


**Fig. 8** The three-dimensional TG-FTIR spectra of PUUA (**a**) under nitrogen, **b** under air; the two-dimensional TG-FTIR spectra of PUUA (**c**) under nitrogen, (**d**) under air

decomposition of polyamide. Then the peaks of aromatic appeared in the temperature range of 623-783 K. It implied the rupture of the bond of polyurea. The results suggested that the order of thermal stability of bonds was like this: polyurethane

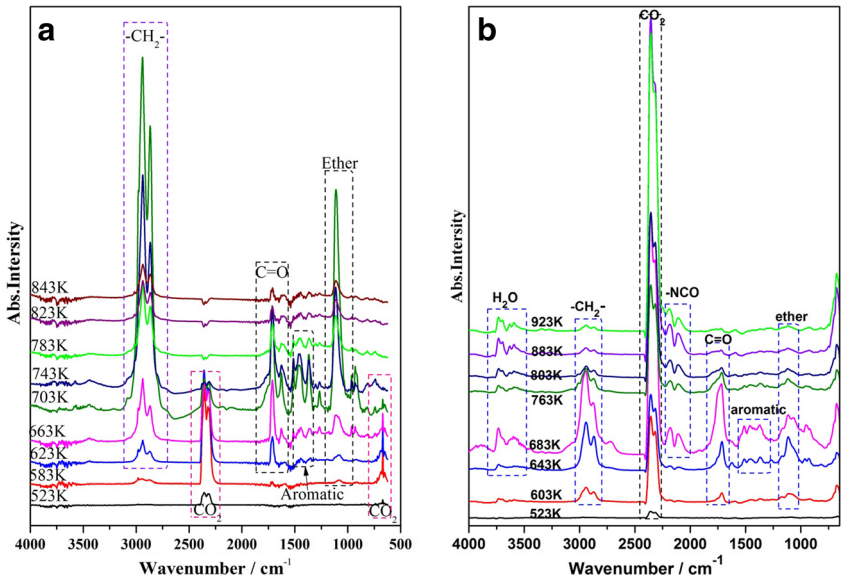


**Fig. 9** The TG-FTIR spectra of PUUA at different temperature (**a**) under nitrogen, (**b**) under air

< polyamide < polyurea. And combining the TG results, the activation energy of PUUA decomposition decreased from 40% mass loss. The temperature of 40% mass loss was 685 K at 10 K/min, which implied that activation energy of the rupture of polyurea was lowest. The decomposition process under nitrogen was showed in Scheme 2.

As the Figs. 8b, d and 9b illustrated, in the whole decomposition process under air, the strongest intensity peak was at

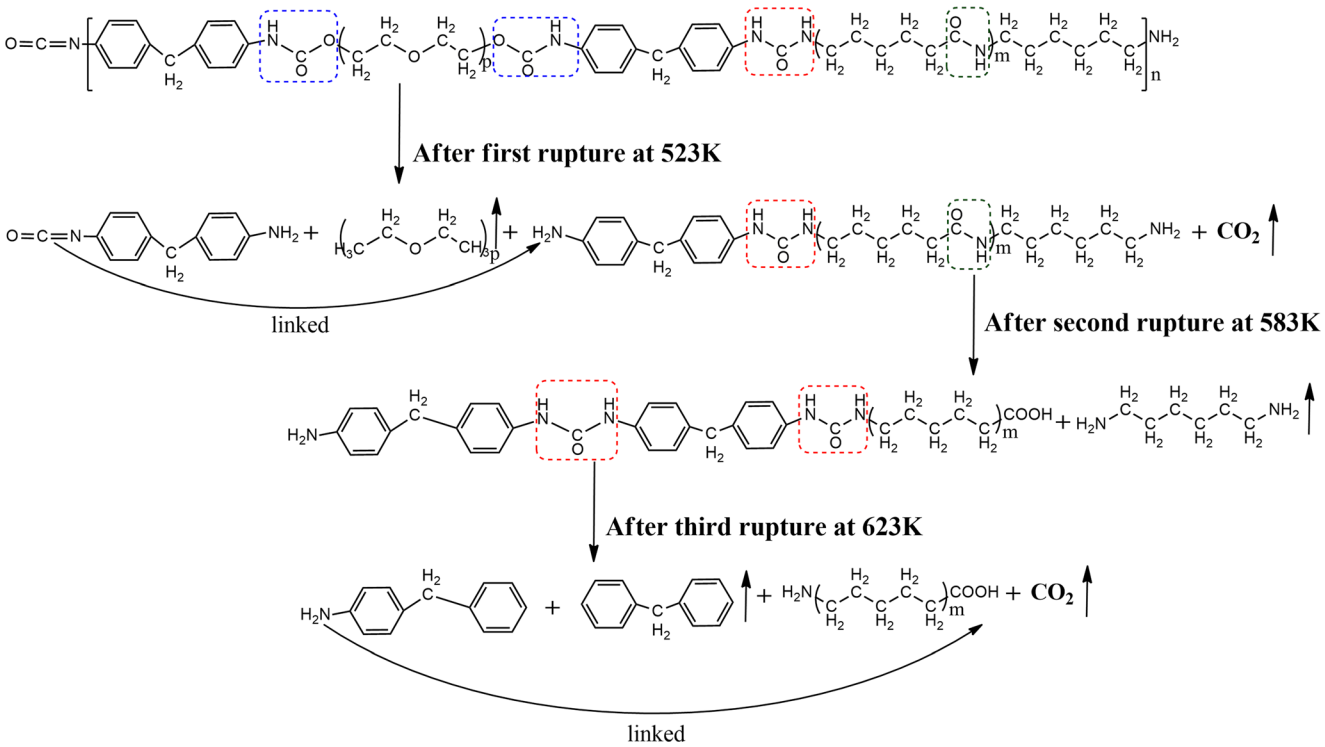


**Scheme 2** The thermal stability order of bonds (in the blue block was bond of polyurethane; in the red block was bond of polyurea; in the green block was bond of polyamide) under nitrogen

2351 $cm^{-1}$ which belonged to $CO_2$. There were also some weak absorption peaks of ether in the range of 2950-2750 $cm^{-1}$ and 1200–1000 $cm^{-1}$ from the temperature of 603 K. It was noticeable that the participation of oxygen shifted the rupture of the bond of polyurethane to low temperature. And combining the TG results under air, the activation energy of PUUA decomposition decreased from 20% mass loss. The temperature of 20% mass loss was 620 K at 10 K/min, which implied that activation energy of the rupture of polyurethane was lowest. It suggested that the rupture of polyurethane was the first rupture with lowest activation energy. And this was different from the results of TG under nitrogen.

There were the characteristic peaks of gaseous $H_2O$ from the temperature of 643 K, which was due to the participation of oxygen. Then in the temperature of 643-683 K, there were the characteristic peaks of gaseous aromatic, which belonged to the fragment of MDI. At high temperature, new shoulder (2200–2100 $cm^{-1}$) appeared after the generating of aromatic. Those phenomena indicated that the oxygen participated in the decomposition and the bond of polyurethane was ruptured firstly under air. The bonds of polyurea and polyamide were ruptured at the same time. These results demonstrated that the protection of polyurethane bond was very important in the process of production and use. The decomposition process under air was listed in Scheme 3.

## Conclusions

A segmented copolymers (poly(urethane-urea-amide) PUUA) was prepared by amide, urethane and urea, which are capable of forming intermolecular hydrogen bonding to enhance the microphase separated morphology. In order to understand the usage temperature of the material and the protective measures which can be used, we wanted study the thermal stability and degradation process of PUUA. The TG results under nitrogen showed the activation energy of PUUA decomposition decreased with the mass loss increasing before 40% mass loss. It indicated that the decomposition activation energy of PUUA decreased due to the change of stability after the initial degradation. After 40% mass loss, the stability of residues increased with the mass loss. Under air, the activation energy of PUUA decomposition decreased with the mass loss increasing before 20% mass loss. Then the activation energy of PUUA increased rapidly. Those results showed that the addition of oxygen changed the trend of activation energy under air. The difference value between the minimum and maximum decomposition energy under air was 366KJ/mol, which was 2.14 times of that under nitrogen. All the difference behaviors under air indicated that the introduction of oxygen accelerated the initial decomposition and catalyzed the production of stable materials.

The results of TG/FTIR under nitrogen suggested that the order of thermal stability of bonds was like this: polyurethane < polyamide < polyurea. And combining the TG results, the temperature of 40% mass loss was 685 K at 10 K/min. The polyurea bonds decomposed at 685 K in TG/FTIR at 10 K/min, which implied that activation energy of polyurea decomposition was lowest. And the phenomena of TG/FTIR under air indicated that the oxygen participated in the decomposition and the bond of polyurethane was ruptured firstly under air. These results demonstrated that the protection of polyurethane bonds was very important in the process of production and use.

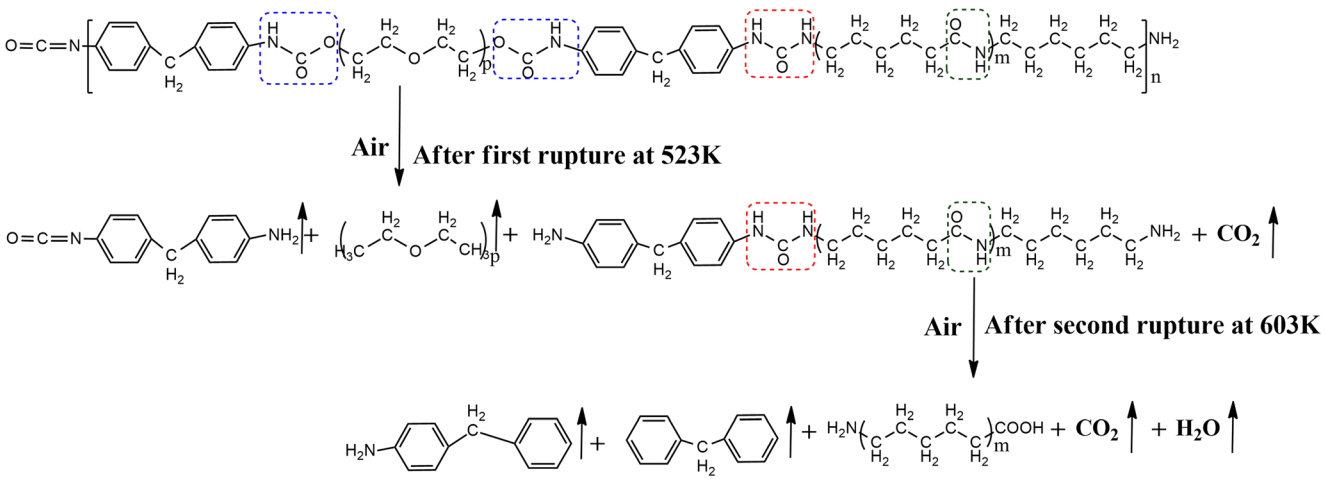


**Scheme 3** The thermal stability order of bonds (in the blue block was bond of polyurethane; in the red block was bond of polyurea; in the green block was bond of polyamide) under air

**Acknowledgements** We would like to thank the generous supports by the Experiment center of Polymer science and engineering academy, Sichuan University, Chengdu, China. We also acknowledge Ms. Rong Zhang of Sichuan University, who helps us analyses the results of TG/FTIR.

## References

1. Beniah G, Uno BE, Tian L et al (2017) Tuning nanophase separation behavior in segmented polyhydroxyurethane via judicious choice of soft segment[J]. Polymer 110:218–227
2. Bondar VI, Freeman BD, Pinnau I (2015) Gas sorption and characterization of poly(ether-b-amide) segmented block copolymers[J]. Journal of Polymer Science Part B Polymer Physics 37(17):2463–2475
3. Lee HS, Roy A, Badami AS, McGrath JE (2007) Synthesis and characterization of sulfonated poly(arylene ether) polyimide multiblock copolymers for proton exchange membranes[J]. Macromol Res 15(2):160–166
4. Miller JA, Lin SB, Hwang KKS, Wu KS, Gibson PE, Cooper SL (1985) Properties of polyether-polyurethane block copolymers: effects of hard segment length distribution[J]. Macromolecules 18(1): 32–44
5. Mokeev MV, Zuev VV (2015) Rigid phase domain sizes determination for poly(urethane–urea)s by solid-state NMR spectroscopy. Correlation with mechanical properties[J]. Eur Polym J 71:372–379
6. Mihajlovic M, Staropoli M, Appavou MS, Wyss HM, Pyckhout-Hintzen W, Sijbesma RP (2017) Tough supramolecular hydrogel based on strong hydrophobic interactions in a multiblock segmented copolymer[J]. Macromolecules 50:3333–3346
7. Schreiner C, Bridge AT, Hunley MT, Long TE, Green MD (2017) Segmented imidazolium ionenes: solution rheology, thermomechanical properties, and electrospinning[J]. Polymer 114:257–265
8. Luong ND, Le HS, Minna M et al (2016) Synthesis and characterization of castor oil-segmented thermoplastic polyurethane with controlled mechanical properties[J]. Eur Polym J 81:129–137
9. Mizgajski A, Bródka S, Fagiewicz K et al (2010) Natural conditions as a premise for the development of the Poznań urbanised area[J]. Int J Therm Sci 98:156–164
10. Chung YC, Han A, Lee GS et al (2016) The effects of grafting bisphenol a or naphthalene derivative onto polyurethane with respect to shape memory and thermal properties[J]. Macromol Res 24(1):1–4
11. Sheth JP, Klinedinst DB, Wilkes GL, Yilgor I, Yilgor E (2005) Role of chain symmetry and hydrogen bonding in segmented copolymers with monodisperse hard segments[J]. Polymer 46(18): 7317–7322
12. Chattopadhyay DK, Raju KVSN (2007) Structural engineering of polyurethane coatings for high performance applications ☆[J]. Prog Polym Sci 32(3):352–418
13. Kim H, Miura Y, Macosko CW (2010) Graphene/polyurethane nanocomposites for improved gas barrier and electrical conductivity[J]. Chem Mater 22(11):3441–3450
14. Chen JH, Hu DD, Li YD, Meng F, Zhu J, Zeng JB (2018) Castor oil derived poly(urethane urea) networks with reprocessibility and enhanced mechanical properties[J]. Polymer 143:79–86
15. Reis RA, Pereira JHC, Campos ACC, Barboza EM, Delpech MC, Cesar DV, Dahmouche K, Bandeira CF (2018) Waterborne poly(-urethane-urea) gas permeation membranes for CO2/CH4 separation[J]. J Appl Polym Sci 135(11)
16. Buckwalter DJ, Dennis JM, Long TE (2015) Amide-containing segmented copolymers[J]. Prog Polym Sci 45:1–22
17. Sheth JP, Xu J, Wilkes GL (2003) Solid state structure–property behavior of semicrystalline poly(ether- block -amide) PEBAX ®;, thermoplastic elastomers[J]. Polymer 44(3):743–756
18. Krijgsman J, Husken D, Gaymans RJ (2003) Synthesis and properties of thermoplastic elastomers based on PTMO and tetra-amide[J]. Polymer 44(25):7573–7588
19. Kayalvizhi M, Suresh J, Karthik S, Arun A (2016) Synthesis and characterization of MDI and functionalized polystyrene based poly(urethane-urea-amide)[J]. Int J Plast Technol 20(1):128–142
20. Kong W, Yang Y, Liu Z, Jiang L, Zhou C, Lei J (2017) Structure–property relations of nylon-6 and polytetramethylene glycol based multiblock copolymers with microphase separation prepared through reactive processing[J]. Polym Int 66:436–442
21. Kissinger HE (1956) Variation of peak temperature with heating rate in differential thermal analysis[J]. J Res Natl Bur Stand 57(4): 217–221
22. Yao F, Wu Q, Lei Y, Guo W, Xu Y (2008) Thermal decomposition kinetics of natural fibers: activation energy with dynamic thermogravimetric analysis[J]. Polym Degrad Stab 93(1):90–98
23. Goyenola C, Stafström S, Hultman L et al (2016) Structural patterns arising during synthetic growth of fullerene-like Sulfocarbide[J]. J Phys Chem C 116(39):21124
24. Sang MS, Kim SH, Song JK (2009) Thermal decomposition behavior and durability evaluation of thermotropic liquid crystalline polymers[J]. Macromol Res 17(3):149–155
25. Ma Z, Sun Q, Ye J, Yao Q, Zhao C (2016) Study on the thermal degradation behaviors and kinetics of alkali lignin for production of phenolic-rich bio-oil using TGA–FTIR and Py–GC/MS[J]. J Anal Appl Pyrolysis 117:116–124